IEEE Access
Multidisciplinary | Rapid Review | Open Access Journal

Received June 23, 2020, accepted July 2, 2020, date of publication July 10, 2020, date of current version July 22, 2020.

Digital Object Identifier 10.1109/ACCESS.2020.3008437

Spatio-Temporal Alignment and Trajectory Matching for Netted Radar Without Prior Spatial Information and Time Delay

XIAOYU CONG, YUBING HAN, (Member, IEEE), WEIXING SHENG, SHANHONG GUO, AND RENLI ZHANG, (Member, IEEE)

School of Electronic and Optical Engineering, Nanjing University of Science and Technology, Nanjing 210094, China

Corresponding author: Yubing Han (hanyb@njust.edu.cn)

This work was supported in part by the National Natural Science Foundation of China under Grant 61971224.

ABSTRACT For netted radars, a new alignment algorithm without prior spatial information (i.e., locations and attitudes of radars) and time delay is proposed to keep the spatio-temporal alignment. The unknown parameters to be estimated include the rotation matrix, the translation vector and the delay between radar stations in this paper. The minimum error function in unified space and time coordinate system is established based on the target trajectory measured by each radar. Firstly, the alternating spatio-temporal alignment method is used to estimate the spatial and temporal parameters, and its statistical performance is compared to the Cramer-Rao bound. Even under severe conditions in which each radar in the network can only observe part of the trajectory, the proposed algorithm can still be adopted to estimate the alignment parameters and complete the trajectory. Then, a trajectory matching algorithm based on random sample consensus (RANSAC) is proposed for multitarget. The corresponding relationship between trajectories is established through minimizing sum of paired trajectory error, and multitarget trajectories from each radar are matched. Finally, the spatio-temporal parameters are refined by all matched trajectory pairs. Simulation results show that the tracking information from different radars is transformed into a unified coordinate after spatio-temporal alignment. Moreover, the registration error is reduced and the tracking accuracy is improved.

INDEX TERMS Netted radar, spatio-temporal alignment, multiple targets, trajectory matching.

I. INTRODUCTION

Networking is used to collect and fuse the observation information from multiple radar stations. The information obtained from each radar is comprehensively processed, controlled and managed by the central station to achieve more accurate tracking [1]. Moreover, radar networking is an effective means to fight against electronic interference. Information interconnection and system viability are strengthened by using radar networking.

In the real radar networking, the measurements of the same observed target from different sensors may not be synchronized in time. Since the tasks and the environment are different for each sensor, the adopted coordinates are different. Therefore, the measurement data cannot be directly fused, and the information obtained by various radars must be unified in the same space-time background, i.e., spatio-temporal alignment [2].

Spatio-temporal alignment is the premise of data fusion for netted radar. The spatio-temporal alignment affects the accuracy of subsequent data fusion directly, which affects the performance of the radar network. Therefore, it is very important to analyze and research the spatio-temporal alignment process for netted radar. The time error of netted radar is affected by many aspects, including different start time and transmission delay in communication network. Therefore, the problem to be solved in time alignment is to synchronize the multi-source asynchronous data to the same time. It ensures that the inputs of data fusion are the measurements of the same target at the same time. Some temporal alignment methods have been proposed up to now, e.g., least square method [3], optimal linearization approach [4], grid based representation [5]. In order to overcome the asynchronous problem, a priori knowledge of the target motion

The associate editor coordinating the review of this manuscript and approving it for publication was Chengpeng Hao.

This work is licensed under a Creative Commons Attribution 4.0 License. For more information, see https://creativecommons.org/licenses/by/4.0/

model named nearly-constant-velocity motion model was researched in [6]. According to this model, a Bayesian algorithm based on importance sampling for the estimation of the static parameter was proposed in [7]. A novel solution to the multisensor bias estimation problem for asynchronous sensors using common targets of opportunity was provided in [8]. However, the approximation procedure in these approaches requires the sensor biases to be small. In [9], an analogous strategy for multitarget systems was proposed based on probability hypothesis density (PHD).

Moreover, the problem needs to be solved in space alignment is to transform the coordinate systems of different radars into a common one. The systematic error exists in trajectory fusion because of the deviation of radar positions, attitudes and measurements. The space registration is also adopted to estimate and compensate the error. Various algorithms for space alignment have been proposed in many literatures. The Kalman filter (KF) alignment algorithm [10] was used to estimate sensor deviation parameters, and extended Kalman filter (EKF) [11], unscented Kalman filter (UKF) [12] and sparse-grid quadrature Kalman filtering (SGQKF) [13] alignment were proposed for nonlinear model. When the measurement noise is relatively large, the performance of registration algorithm is deteriorated. In order to solve this problem, an exact maximum likelihood (EML) registration algorithm was presented in [14]. Based on EML, a modified exact maximum likelihood (MEML) registration algorithm was proposed in [15]. The performance of MEML in terms of accuracy and convergence are better than the EML algorithm, since the likelihood function is exact with the computation of the covariance of the measurement noise. A hierarchical neural network method was proposed to estimate sensor bias in [16], which was a nonparametric method. A neural extended Kalman filter (NEKF) [17] was proposed to model the sensor systems, which learned the differences between the priori model and the actual model. It takes a long training time to meet the real-time requirements in all neural network-based algorithms. An on-line absolute sensor registration algorithm was proposed to solve the real-time problem for 3-D radars networking in [18]. The difference in the position of the target was used to compute bias parameters. This algorithm was applicable to the situations without radar location errors. In addition, it was assumed that the radars of network are synchronous in time with the same update rates. In [19], an expectation maximization (EM) registration algorithm for multiple radars network was presented. Time bias, angular biases and range bias were estimated using the EM algorithm, and the EM algorithm was incorporated with the KF to estimate parameters in [20]. For multi-target tracking, the probability hypothesis density (PHD) [21], [22] filter has the distinct advantage that it avoids the complicated data association. The associations are usually uncertain in the multi-target tracking scene. The GM-PHD filter [23], which avoided the data association, was used for estimating the systematic bias recursively in multi-target tracking scene.

In [24], a KF based on a linearized alignment model was proposed. Both offset and attitude errors were aligned to solve the relative grid-locking problem for two 3-D radars. This algorithm was under the assumption that the sensors were synchronized in time. The relative location of the two radars was assumed perfectly known in this algorithm, i.e., location errors were not present, which limited the applicability of the algorithm. To solve this problem, a spatial registration method based on least square (LS) was proposed in [25], which estimated and compensated the location, attitude and measurement biases of radar stations. The radar location and attitude biases were allowed in this algorithm. However, the time registration was not taken into account in the data model as well. Thus, the algorithm was effective with the assumption that the measurements were time synchronous.

Most of the current radar information alignment algorithms are separately designed in the time domain and space domain, without considering the relationship between spatial alignment and temporal alignment. Moreover, prior spatial information and time synchronization are required. If the time and space parameters can be aligned simultaneously without prior spatial information (including locations, attitudes of radar stations) and time delay, the alignment error caused by the prior information biases can be avoided. The time and space alignment parameters can be estimated to reduce the error of radar information fusion, and the application range of the algorithm is expanded.

In this paper, a new algorithm is proposed to estimate the spatio-temporal alignment parameters for the netted radar without prior spatial information and time delay. When the prior spatial information (including locations and attitudes of radar stations) are unknown, the rotation matrix and the translation vector between radar stations are the alignment parameters to be estimated. In time alignment, the measurement cycle of each radar is known in most cases for netted radars. Therefore, the main unknown time parameter is the delay caused by the discrepant clock reference of the radars. In this paper, the unknown parameters to be estimated include the rotation matrix, translation vector and the delay between radar stations. Those parameters are obtained based on the target trajectory in the proposed algorithm. In unified space and time coordinate system, the minimum error function is established to estimate and compensate alignment parameters. The minimization is performed by alternative iterate method to estimate the spatial and temporal parameters. Unlike previous works, the spatio-temporal alignment method does not require prior spatial information and time delay of radar stations. Moreover, the Cramer-Rao lower bound (CRLB) is derived for the radar alignment algorithm. The tracking error after registration and fusion is reduced. Furthermore, in severe cases, the radars can only observe part of the target trajectory because of electronic jamming. The proposed algorithm can be used to estimate spatio-temporal alignment parameters to reconstruct the complete trajectory. This method reduces the influence of interference on target tracking. Based on the new

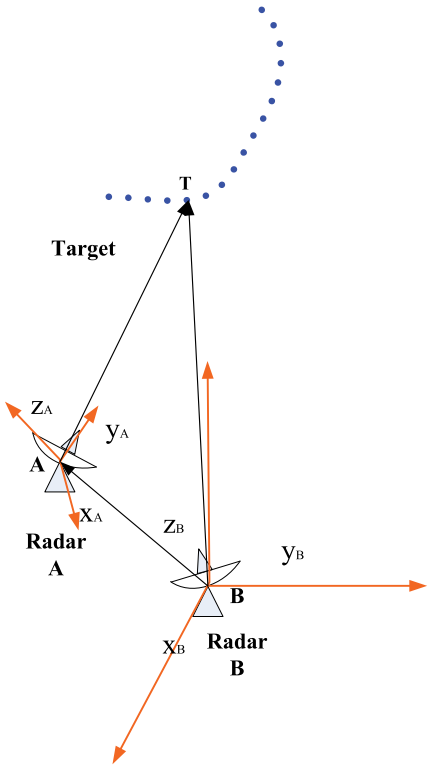

FIGURE 1. Spatio-Temporal Alignment Problem.

alignment method, a spatio-temporal alignment and matching algorithm based on RANSAC is proposed for multi-target tracking. The multiple target trajectories from different radar stations are matched through minimizing sum of paired trajectory error. The estimated time and space alignment parameters are obtained according to all matched trajectory pairs. The multi-target trajectories measured by multiple radars are correctly matched, and multi-target tracking accuracy is improved after spatio-temporal alignment.

The rest of paper is organized as follows. Sections II formulates the problem of spatio-temporal alignment for single target trajectory. Section III shows the simulation and analysis for single target. Section IV presents matching and alignment for multiple target trajectories. Finally, some concluding remarks are reported in Section V.

II. SPATIO-TEMPORAL ALIGNMENT FOR SINGLE TARGET

A. ALTERNATING SPATIO-TEMPORAL ALIGNMENT METHOD

The geometry of the scenario is shown in Fig. 1. Two radars are taken as an example.

$\mathbf{p}(t) = [x_A(t), y_A(t), z_A(t)]^T$ is the position vector of the target in A coordinate system at time t.

$\mathbf{q}(t) = [x_B(t), y_B(t), z_B(t)]^T$ is the position vector of the target in B coordinate system at time t.

From the geometry of the problem, shown in Fig. 1, the following relation holds

$$\mathbf{q}(t) = \mathbf{H} \cdot \mathbf{p}(t) + \mathbf{c} \tag{1}$$

where $\mathbf{H}$ is a 3×3 rotation matrix of angles α,β and γ that aligns the radar A reference frame to the radar B reference frame. Matrix $\mathbf{H}$ is given by (2), as shown at the bottom of the page.

And $\mathbf{c}$ is a 3×1 translation vector expressed as $\mathbf{c} = [c_1, c_2, c_3]^T$.

In consideration of asynchronization and noise, the relation of measurements from radar A and radar B is expressed as

$$\mathbf{q}(t') = \mathbf{H} \cdot \mathbf{p}(t) + \mathbf{c} + \boldsymbol{\varepsilon} \tag{3}$$

where $\boldsymbol{\varepsilon}$ represents the zero-mean Gaussian error. Note that $t' = s \cdot t + \Delta t$, where s is the ratio between measurement cycles of the two radars. Since measurement cycles of radars are known in practice, s is known in most cases. Δt is the delay.

Assume that $\mathbf{p}(t) = [x_A(t), y_A(t), z_A(t)]^T$ is the target trajectory from radar A, and $\mathbf{q}(t')=[x_B(t'), y_B(t'), z_B(t')]^T$ is the corresponding space-time point from radar B.

The spatio-temporal alignment for single target can be formulated as the optimization problem

$$(\mathbf{H}, \mathbf{c}, \Delta t) = \arg\min_{\mathbf{H},\mathbf{c},\Delta t} \sum_{i=1}^{N} \|\mathbf{q}(s \cdot t_i + \Delta t) - (\mathbf{H} \cdot \mathbf{p}(t_i) + \mathbf{c})\|^2 \tag{4}$$

where $\mathbf{H}$ is a 3×3 rotation matrix, $\mathbf{c}$ is a 3×1 translation vector, t_i is the i-th moment and N is the number of measurements. The minimization problem can be solved by alternating the following two steps until the algorithm converges to obtain the optimal solution to (4).

1) Spatial alignment: Δt is fixed and singular value decomposition (SVD) is adopted to solve $\mathbf{H}$ and $\mathbf{c}$.

2) Temporal alignment: $\mathbf{H}$ and $\mathbf{c}$ are fixed, and we solve Δt by fitting the best linear interpolation value.

B. SPATIAL ALIGNMENT

For convenience, let $\mathbf{p}(t_i) = \mathbf{p}_i$, $\mathbf{q}(s \cdot t_i + \Delta t) = \mathbf{q}_i$, spatial alignment function can be expressed as

$$(\mathbf{H}, \mathbf{c}) = \arg\min_{\mathbf{H},\mathbf{c}} \sum_{i=1}^{N} \|\mathbf{q}_i - (\mathbf{H} \cdot \mathbf{p}_i + \mathbf{c})\|^2 \tag{5}$$

$$\mathbf{H} = \begin{bmatrix} \cos\alpha\cos\beta & cos\alpha sin\beta sin\gamma - sin\alpha cos\gamma & cos\alpha sin\beta cos\gamma + sin\alpha sin\gamma \\ \sin\alpha\cos\beta & sin\alpha sin\beta sin\gamma + cos\alpha cos\gamma & sin\alpha sin\beta cos\gamma - cos\alpha sin\gamma \\ -\sin\beta & cos\beta sin\gamma & cos\beta cos\gamma \end{bmatrix} \tag{2}$$

Let $F = \sum_{i=1}^{N} \|\mathbf{q}_i - (\mathbf{H} \cdot \mathbf{p}_i + \mathbf{c})\|^2$ and take the partial derivative with respect to $\mathbf{c}$, we have

$$\frac{\partial F}{\partial \mathbf{c}} = 2\mathbf{c}N + 2\mathbf{H}\left(\sum_{i=1}^{N} \mathbf{p}_i\right) - 2\sum_{i=1}^{N} \mathbf{q}_i \tag{6}$$

Let $\frac{\partial F}{\partial \mathbf{c}} = 0$, and we have

$$\mathbf{c} = \frac{1}{N}\sum_{i=1}^{N} \mathbf{q}_i - \mathbf{H} \cdot \frac{1}{N}\sum_{i=1}^{N} \mathbf{p}_i \tag{7}$$

We define $\bar{\mathbf{p}} = \frac{1}{N}\sum_{i=1}^{N} \mathbf{p}_i$ and $\bar{\mathbf{q}} = \frac{1}{N}\sum_{i=1}^{N} \mathbf{q}_i$, then

$$\mathbf{c} = \bar{\mathbf{q}} - \mathbf{H} \cdot \bar{\mathbf{p}} \tag{8}$$

Therefore

$$\sum_{i=1}^{N} \|(\mathbf{H} \cdot \mathbf{p}_i + \mathbf{c}) - \mathbf{q}_i\|^2 = \sum_{i=1}^{N} \|\mathbf{H} \cdot (\mathbf{p}_i - \bar{\mathbf{p}}) - (\mathbf{q}_i - \bar{\mathbf{q}})\|^2 \tag{9}$$

Assume $\mathbf{a}_i = \mathbf{p}_i - \bar{\mathbf{p}}$ and $\mathbf{b}_i = \mathbf{q}_i - \bar{\mathbf{q}}$, $\mathbf{H}$ can be obtained by

$$\mathbf{H} = \arg\min_{\mathbf{H}} \sum_{i=1}^{N} \|\mathbf{H} \cdot \mathbf{a}_i - \mathbf{b}_i\|^2 \tag{10}$$

(10) is expanded to minimize

$$\begin{aligned} J &= \sum_{i=1}^{N} \|\mathbf{H} \cdot \mathbf{a}_i - \mathbf{b}_i\|^2 \\ &= \sum_{i=1}^{N} (\mathbf{H} \cdot \mathbf{a}_i - \mathbf{b}_i)^T (\mathbf{H} \cdot \mathbf{a}_i - \mathbf{b}_i) \\ &= \sum_{i=1}^{N} \left(\mathbf{a}_i^T \mathbf{a}_i - 2\mathbf{b}_i^T \mathbf{H} \mathbf{a}_i + \mathbf{b}_i^T \mathbf{b}_i\right) \end{aligned} \tag{11}$$

Therefore, the minimization problem in (10) is equivalent to maximize

$$W = \sum_{i=1}^{N} \mathbf{b}_i^T \mathbf{H} \mathbf{a}_i = tr\left(\mathbf{B}^T \mathbf{H} \mathbf{A}\right) \tag{12}$$

where $\mathbf{A} = [\mathbf{a}_1, \mathbf{a}_2, \ldots \mathbf{a}_N]$ and $\mathbf{B} = [\mathbf{b}_1, \mathbf{b}_2, \ldots \mathbf{b}_N]$. According to the commutative law for matrix trace, we get

$$W = tr(\mathbf{B}^T \mathbf{H} \mathbf{A}) = tr\left(\mathbf{H} \mathbf{A} \mathbf{B}^T\right) \tag{13}$$

Let $\mathbf{S} = \mathbf{A}\mathbf{B}^T$, and the SVD of $\mathbf{S}$ can be expressed as

$$\mathbf{S} = \mathbf{U}\mathbf{\Sigma}\mathbf{V}^T \tag{14}$$

By inserting (14) in (13), we obtain

$$tr\,(\mathbf{H}\mathbf{S}) = tr\left(\mathbf{H}\mathbf{U}\mathbf{\Sigma}\mathbf{V}^T\right) = tr\left(\mathbf{\Sigma}\mathbf{V}^T\mathbf{H}\mathbf{U}\right) \tag{15}$$

where $\mathbf{U}$ and $\mathbf{V}$ are orthogonal matrices and $\mathbf{\Sigma}$ is a diagonal matrix. Since $\mathbf{U}$, $\mathbf{H}$, $\mathbf{V}$ are all orthogonal matrices, $\mathbf{M} = \mathbf{V}^T\mathbf{H}\mathbf{U}$ is also an orthogonal matrix. That is, $\mathbf{M} \cdot \mathbf{M}^T = \mathbf{I}$. We define that m_{ij} is entry of $\mathbf{M}$ and m_j is the column of $\mathbf{M}$. We have

$$\sum_{i=1}^{k} m_{ij}^2 = m_j^T m_j = 1 \tag{16}$$

Therefore

$$\left|m_{ij}\right| \leq 1 \tag{17}$$

(15) can be rewritten as

$$\begin{aligned} tr\,(\mathbf{\Sigma}\mathbf{M}) &= \begin{pmatrix} \sigma_1 & & & \\ & \sigma_2 & & \\ & & \ddots & \\ & & & \sigma_k \end{pmatrix} \begin{pmatrix} m_{11} & m_{12} & \cdots & m_{1k} \\ m_{21} & m_{22} & \cdots & m_{2k} \\ \vdots & \vdots & \vdots & \vdots \\ m_{k1} & m_{k2} & \cdots & m_{kk} \end{pmatrix} \\ &= \sum_{i=1}^{k} \sigma_i m_{ii} \end{aligned} \tag{18}$$

$\sigma_1, \sigma_2, \sigma_3 \cdots, \sigma_k$ are diagonal elements of diagonal matrix $\mathbf{\Sigma}$. And $\sigma_1 \geq \sigma_2 \geq \sigma_3 \cdots \geq \sigma_k \geq 0$. Therefore, we can make m_{ii} equal to 1 to obtain the maximum trace. Since $\mathbf{M}$ is also an orthogonal matrix, $\mathbf{M}$ is an identity matrix. Therefore

$$\mathbf{V}^T\mathbf{H}\mathbf{U} = \mathbf{M} = \mathbf{I} \tag{19}$$

Now we get

$$\mathbf{H} = \mathbf{V}\mathbf{U}^T \tag{20}$$

In (20), if $\det(\mathbf{V}\mathbf{U}^T) = +1$, $\mathbf{H}$ is a rotation matrix which is the desired solution. If $\det(\mathbf{V}\mathbf{U}^T) = -1$, then it is a reflection matrix.

Assuming $\det(\mathbf{V}\mathbf{U}^T) = -1$, we search for $\mathbf{M}$ that maximizes

$$tr(\mathbf{\Sigma}\mathbf{M}) = \sigma_1 m_{11} + \sigma_2 m_{22} + \ldots + \sigma_k m_{kk} \tag{21}$$

Apparently, all of m_{ii} take 1 to get the maximum extreme. But that value has to be excluded (The $\mathbf{H}$ obtained from this is the reflection matrix), the sub-optimal value $(m_{11}, \ldots, m_{kk})$ is (1, 1, …, 1, -1) [26].

$$tr(\mathbf{\Sigma}\mathbf{M}) = \sigma_1 + \sigma_2 + \ldots + \sigma_{k-1} - \sigma_k \tag{22}$$

Therefore, we have

$$\mathbf{M} = \begin{cases} \mathbf{I} & \det\left(\mathbf{V}\mathbf{U}^T\right) = +1 \\ diag\,(1, \ldots, 1, -1) & \det\left(\mathbf{V}\mathbf{U}^T\right) = -1 \end{cases} \tag{23}$$

We can rewrite a general formula, which encompasses both cases of $\det\left(\mathbf{V}\mathbf{U}^T\right) = +1$ and $\det\left(\mathbf{V}\mathbf{U}^T\right) = -1$

$$\mathbf{H} = \mathbf{V}\begin{pmatrix} 1 & & & \\ & 1 & & \\ & & \ddots & \\ & & & 1 \\ & & & & \det\left(\mathbf{V}\mathbf{U}^T\right) \end{pmatrix}\mathbf{U}^T \tag{24}$$

The translation vector $\mathbf{c}$ is obtained by

$$\mathbf{c} = \bar{\mathbf{q}} - \mathbf{H} \cdot \bar{\mathbf{p}} \tag{25}$$

C. TEMPORAL ALIGNMENT

In this section, we discuss the time alignment with fixed $\mathbf{H}$ and $\mathbf{c}$. It is assumed that that $\mathbf{p}(t) = [x_A(t), y_A(t), z_A(t)]^T$ is the target trajectory from radar A, $\mathbf{q}(t') = \left[x_B(t'), y_B(t'), z_B(t')\right]^T$ is the corresponding space-time point from radar B, and $t' = s \cdot t + \Delta t$. Since t' is not always an integer, it is interpolated from the adjacent point (integer time) locations: $t_L = \lfloor t' \rfloor$, $t_H = \lceil t' \rceil$, where $\lfloor\rfloor$ and $\lceil\rceil$ are the round operators towards minus and plus infinity.

$$\mathbf{q}(t') = \mathbf{q}(t_L) \cdot \left(1 - \frac{t' - t_L}{t_H - t_L}\right) + \mathbf{q}(t_H) \cdot \frac{t' - t_L}{t_H - t_L} \tag{26}$$

that is

$$\mathbf{q}(s \cdot t + \Delta t) = \mathbf{q}(t_L) \cdot \left(1 - \frac{s \cdot t + \Delta t - t_L}{t_H - t_L}\right) + \mathbf{q}(t_H) \cdot \frac{s \cdot t + \Delta t - t_L}{t_H - t_L} \tag{27}$$

Thus temporal alignment can be expressed as

$$\Delta t = \arg\min_{\Delta t} \sum_{i=1}^{N} \left\| \mathbf{q}(t_L) \cdot \left(1 - \frac{s \cdot t_i + \Delta t - t_L}{t_H - t_L}\right) + \mathbf{q}(t_H) \cdot \frac{s \cdot t_i + \Delta t - t_L}{t_H - t_L} - (\mathbf{H} \cdot \mathbf{p}(t_i) + \mathbf{c}) \right\|^2 \tag{28}$$

From (28),

$$\Delta t = \left(\sum_{i=1}^{N} \mathbf{A}^T \mathbf{A}\right)^{-1} \left(\sum_{i=1}^{N} \mathbf{A}^T \mathbf{b}\right) \tag{29}$$

where $\mathbf{A} = \frac{1}{t_H - t_L}[\mathbf{q}(t_H) - \mathbf{q}(t_L)]$, $\mathbf{b} = \mathbf{H} \cdot \mathbf{p}(t_i) + \mathbf{c} - \mathbf{q}(t_L) + (\mathbf{q}(t_L) - \mathbf{q}(t_H)) \frac{s \cdot t_i - t_L}{t_H - t_L}$.

The pseudo-code of spatio-temporal alignment algorithm is shown in Algorithm 1.

D. THE Cramer–Rao LOWER Bound(CRLB) FOR ALIGNMENT

In this section, the detailed derivation of the CRLB is given for the radar alignment algorithm.

(3) can be expressed as

$$\mathbf{q} = \mathbf{H}\mathbf{p} + \mathbf{c} + \boldsymbol{\varepsilon} \tag{30}$$

From (2), $\mathbf{H}$ is a 3×3 rotation matrix of angles α, β and γ that aligns the radar A reference frame to the radar B reference frame. And $\mathbf{c}$ is a 3×1 vector. Therefore suppose

$$\boldsymbol{\theta} = [\alpha, \beta, \gamma]^T \tag{31}$$
$$\mathbf{c} = [c_1, c_2, c_3]^T \tag{32}$$

To evaluate the CRLB, we need to know the likelihood function that can be expressed as

$$p(\mathbf{q}|\boldsymbol{\theta}, \mathbf{c}) \propto \exp\left\{-\frac{1}{2}\sum_{i=1}^{N} [\mathbf{q}_i - \mathbf{H}(\boldsymbol{\theta})\mathbf{p}_i - \mathbf{c}]^T \mathbf{R}^{-1} [\mathbf{q}_i - \mathbf{H}(\boldsymbol{\theta})\mathbf{p}_i - \mathbf{c}]\right\} \tag{33}$$

where $\mathbf{R}$ is the covariance matrix.

Algorithm 1 Spatio-Temporal Alignment Algorithm

Require:
Target trajectory from radar A: $\mathbf{p}$;
Target trajectory from radar B: $\mathbf{q}$;
Ensure:
Rotation matrix: $\mathbf{H}$;
Translation vector: $\mathbf{c}$;
Delay: Δt;

```
loop
    Compute mean value of trajectories
    p̄ = (1/N) Σ_{i=1}^{N} p_i
    q̄ = (1/N) Σ_{i=1}^{N} q_i
    Assume a_i = p_i − p̄ and b_i = q_i − q̄;
    Let S = AB^T, where A = [a_1, a_2, ... a_N] and B = [b_1, b_2, ... b_N];
    Compute the SVD of S
    S = UΣV^T
    Compute H as in (24)
    c = q̄ − H · p̄
    Compute the delay Δt as in (29)
    Update φ = Σ_{i=1}^{N} ||(H · p_i + c) − q_i||^2
end loop
return H, c, Δt;
```

Suppose

$$\begin{aligned}\lambda &= -\ln p(\mathbf{q}|\boldsymbol{\theta}, \mathbf{c}) \\ &\propto \frac{1}{2}\sum_{i=1}^{N} [\mathbf{q}_i - \mathbf{H}(\boldsymbol{\theta})\mathbf{p}_i - \mathbf{c}]^T \mathbf{R}^{-1} [\mathbf{q}_i - \mathbf{H}(\boldsymbol{\theta})\mathbf{p}_i - \mathbf{c}] \\ &= \frac{1}{2}\sum_{i=1}^{N} [\mathbf{q}_i - \mathbf{g}_i - \mathbf{c}]^T \mathbf{R}^{-1} [\mathbf{q}_i - \mathbf{g}_i - \mathbf{c}]\end{aligned} \tag{34}$$

where $\mathbf{g}_i = \mathbf{H}(\boldsymbol{\theta})\mathbf{p}_i$. In order to handle complicated derivation, we adopt the tools for finding derivatives in [27]. In this way, the gradient of λ can be expressed as

$$[\nabla_{\boldsymbol{\theta}}\lambda]_{3\times 1} = (D_{\boldsymbol{\theta}}\lambda)^T \tag{35}$$
$$[\nabla_{\mathbf{c}}\lambda]_{3\times 1} = (D_{\mathbf{c}}\lambda)^T \tag{36}$$

In order to solve the $D_{\boldsymbol{\theta}}\lambda$ and $D_{\mathbf{c}}\lambda$, $d\lambda$ is rewritten by the following differential expression

$$\begin{aligned}d\lambda &= \frac{1}{2}\sum_{i=1}^{N} \{d[\mathbf{q}_i - \mathbf{g}_i - \mathbf{c}]^T \mathbf{R}^{-1} [\mathbf{q}_i - \mathbf{g}_i - \mathbf{c}] \\ &\quad + [\mathbf{q}_i - \mathbf{g}_i - \mathbf{c}]^T \mathbf{R}^{-1} d[\mathbf{q}_i - \mathbf{g}_i - \mathbf{c}]\} \\ &= -\frac{1}{2}\sum_{i=1}^{N} \{[d\mathbf{g}_i + d\mathbf{c}]^T \mathbf{R}^{-1} [\mathbf{q}_i - \mathbf{g}_i - \mathbf{c}] \\ &\quad + [\mathbf{q}_i - \mathbf{g}_i - \mathbf{c}]^T \mathbf{R}^{-1} d[\mathbf{g}_i + \mathbf{c}]\} \\ &= -\sum_{i=1}^{N} [\mathbf{q}_i - \mathbf{g}_i - \mathbf{c}]^T \mathbf{R}^{-1} d[\mathbf{g}_i + \mathbf{c}]\end{aligned} \tag{37}$$

From (37),

$$D_{\mathbf{g}_i}\lambda = [\mathbf{g}_i - \mathbf{q}_i + \mathbf{c}]^T \mathbf{R}^{-1} \tag{38}$$

$$D_{\mathbf{c}}\lambda = \sum_{i=1}^{N} [\mathbf{g}_i - \mathbf{q}_i + \mathbf{c}]^T \mathbf{R}^{-1} \tag{39}$$

Since we can't get $D_{\boldsymbol{\theta}}\lambda$ directly, we use the chain rule to factorize $D_{\boldsymbol{\theta}}\lambda$ into the expression of $D_{\mathbf{g}_i}\lambda$, $D_{\mathbf{H}}\mathbf{g}_i$ and $D_{\boldsymbol{\theta}}\mathbf{H}$.

$$D_{\boldsymbol{\theta}}\lambda = \left(\sum_{i=1}^{N} D_{\mathbf{g}_i}\lambda \cdot D_{\mathbf{H}}\mathbf{g}_i\right) D_{\boldsymbol{\theta}}\mathbf{H} \tag{40}$$

$D_{\mathbf{g}_i}\lambda$ has been obtained in (38), and we need to deduce $D_{\mathbf{H}}\mathbf{g}_i$ and $D_{\boldsymbol{\theta}}\mathbf{H}$. To obtain $D_{\mathbf{H}}\mathbf{g}_i$, $d\mathbf{g}_i$ is expressed as

$$d\mathbf{g}_i = (d\mathbf{H})\,\mathbf{p}_i = ((p_i(1), p_i(2), p_i(3)) \otimes \mathbf{I}_3)\,(dvec(\mathbf{H})) \tag{41}$$

where the vectorization operator $vec(\cdot)$ stacks the columns vectors of the argument matrix into a long column vector in chronological order. From (41),

$$D_{\mathbf{H}}\mathbf{g}_i = ((p_i(1), p_i(2), p_i(3)) \otimes \mathbf{I}_3) \tag{42}$$

To obtain $D_{\boldsymbol{\theta}}\mathbf{H}$, $dvec(\mathbf{H})$ is expressed as (43), as shown at the bottom of the page, where expression of $\mathbf{A}(\alpha, \beta, \gamma)$ is shown in (44), as shown at the bottom of the page. Therefore

$$D_{\boldsymbol{\theta}}\mathbf{H} = \mathbf{A}(\alpha, \beta, \gamma) \tag{45}$$

By making use of (38), (42), and (45), (40) can be rewritten as

$$D_{\boldsymbol{\theta}}\lambda = \left(\sum_{i=1}^{N} \left([\mathbf{g}_i - \mathbf{q}_i - \mathbf{c}]^T \mathbf{R}^{-1}\right) ((p_i(1), p_i(2), p_i(3)) \otimes \mathbf{I}_3)\right) \cdot \mathbf{A}(\alpha, \beta, \gamma) \tag{46}$$

The CRLB for parameters $\boldsymbol{\theta}$ and $\mathbf{c}$ are expressed as the tools for finding derivatives in [27].

$$CRLB(\boldsymbol{\theta}) = \frac{1}{(\Delta_{\boldsymbol{\theta}}\lambda)\,(\Delta_{\boldsymbol{\theta}}\lambda)^T} = \frac{1}{(D_{\boldsymbol{\theta}}\lambda)^T\,(D_{\boldsymbol{\theta}}\lambda)} \tag{47}$$

$$CRLB(\mathbf{c}) = \frac{1}{(\Delta_{\mathbf{c}}\lambda)\,(\Delta_{\mathbf{c}}\lambda)^T} = \frac{1}{(D_{\mathbf{c}}\lambda)^T\,(D_{\mathbf{c}}\lambda)} \tag{48}$$

According to $D_{\boldsymbol{\theta}}\lambda$ in (46) and $D_{\mathbf{c}}\lambda$ in (39), the CRLB for parameters $\boldsymbol{\theta}$ and $\mathbf{c}$ can be obtained.

III. SIMULATION AND ANALYSIS FOR SINGLE TARGET

Linear frequency modulation (LFM) waveform of X band is used for simulations and analysis. The time-bandwidth product of the LFM waveform is 24. The radar A in the geodetic coordinates is [200; 300; 500]. Each measurement cycle contains 4 kinds of LFM waveform with different pulse length (used for solving ambiguity resolution in range and velocity). The measurement cycle is called coherent processing intervals (CPI), and each CPI contains 256 pulse repetition intervals (PRI). The period of a measurement point is 18.7ms. The radar B in the geodetic coordinates is [300; 450; 780]. Each measurement cycle contains 4 kinds of LFM waveform with different pulse length, and each CPI contains 288 PRIs. The period of a measurement point is 21.0ms. Thus, the ratio between measurement cycle of the radar A and B is $s = 8/9$. The radar B has a delay of $\Delta t = 5ms$ compared with radar A. Radar A and radar B are characterized by the following measured parameters: i) range accuracy: $\sigma_{\rho,A} = \sigma_{\rho,B} = 1\,m$; ii) azimuth accuracy: $\sigma_{\theta,A} = \sigma_{\theta,B} = 0.01°$; and iii) elevation accuracy: $\sigma_{\varepsilon,A} = \sigma_{\varepsilon,B} = 0.01°$. A single target flies along a certain non-linear trajectory. Radar A and radar B get the target trajectories $\mathbf{p}(t)$ and $\mathbf{q}(t')$ in their spatio-temporal coordinates, respectively, as shown in Fig.2. $\mathbf{p}(t)$ and $\mathbf{q}(t')$ are N pairs of measurements coming from the same target. In our simulations, $N = 100$. The target is maneuverable, and it has an acceleration of 60 m/s^2 in the positive direction of the Y-axis and 60 m/s^2 in the positive direction of the Z-axis.

Fig.2 shows that the trajectories of radar A and radar B are totally different, which are directly obtained in the spatio-temporal coordinates of different radars. Data fusion cannot be completed if time and space are not aligned. In the absence of prior spatial information and time delay of radar A and B, the space and time registration parameters ($\mathbf{H}$, $\mathbf{c}$, Δt) can be estimated by using the proposed algorithm based on

$$dvec(\mathbf{H}) = vec\begin{bmatrix} d(\cos\alpha\cos\beta) & d(cos\alpha sin\beta sin\gamma - sin\alpha cos\gamma) & d(cos\alpha sin\beta cos\gamma + sin\alpha sin\gamma) \\ d(\sin\alpha\cos\beta) & d(sin\alpha sin\beta sin\gamma + cos\alpha cos\gamma) & d(sin\alpha sin\beta cos\gamma - cos\alpha sin\gamma) \\ d(\sin\beta) & d(cos\beta sin\gamma) & d(cos\beta cos\gamma) \end{bmatrix} = \mathbf{A}(\alpha, \beta, \gamma)\begin{pmatrix} d\alpha \\ d\beta \\ d\gamma \end{pmatrix} \tag{43}$$

$$\mathbf{A}(\alpha, \beta, \gamma) = \begin{bmatrix} -\sin\alpha\cos\beta & -cos\alpha sin\beta & 0 \\ cos\alpha cos\beta & -sin\alpha sin\beta & 0 \\ 0 & cos\beta & 0 \\ -sin\alpha sin\beta sin\gamma - \cos\alpha\cos\gamma & cos\alpha cos\beta sin\gamma & cos\alpha sin\beta\cos\gamma + sin\alpha\sin\gamma \\ \cos\alpha sin\beta sin\gamma - \sin\alpha cos\gamma & sin\alpha\cos\beta sin\gamma & sin\alpha sin\beta\cos\gamma - cos\alpha\sin\gamma \\ 0 & -sin\beta sin\gamma & cos\beta\cos\gamma \\ -\sin\alpha sin\beta cos\gamma + cos\alpha sin\gamma & cos\alpha\cos\beta cos\gamma & -cos\alpha sin\beta\sin\gamma + sin\alpha\cos\gamma \\ \cos\alpha sin\beta cos\gamma + \sin\alpha sin\gamma & sin\alpha\cos\beta cos\gamma & -sin\alpha sin\beta\sin\gamma - cos\alpha\cos\gamma \\ 0 & -sin\beta cos\gamma & -cos\beta sin\gamma \end{bmatrix} \tag{44}$$

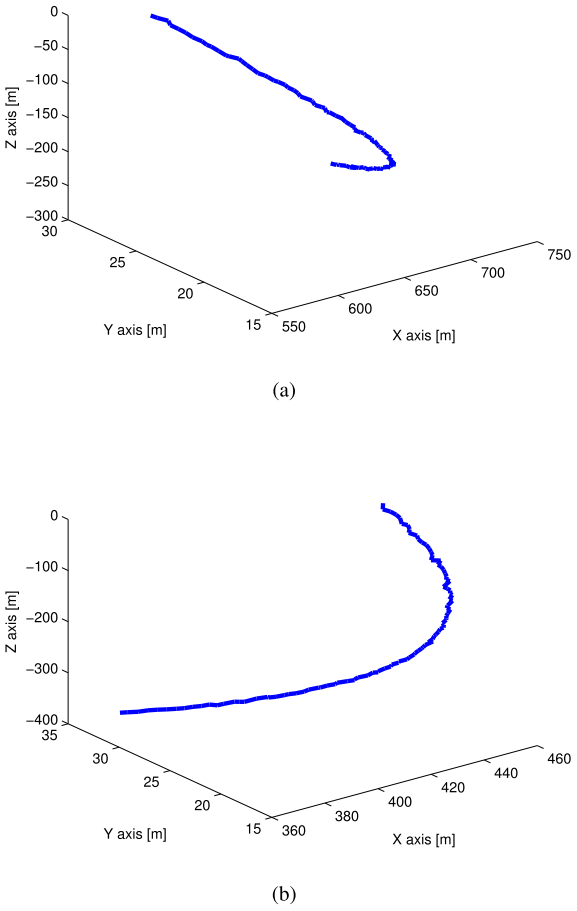

FIGURE 2. Target trajectory before spatio-temporal alignment. (a) From radar A (b) From radar B.

the trajectories $\mathbf{p}(t)$ and $\mathbf{q}(t')$. The measurements from radar A after spatial and temporal alignment are shown in Fig. 3.

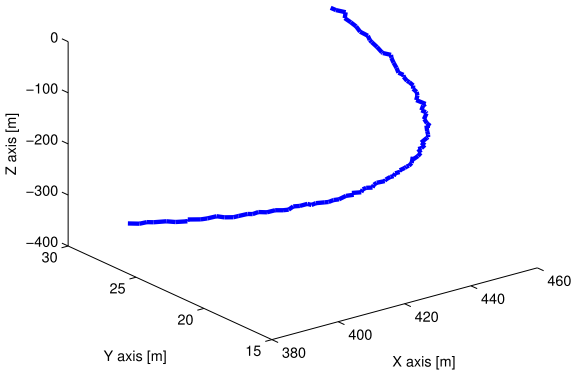

FIGURE 3. Target trajectory from radar A after spatio-temporal alignment.

From Fig.2(b) and Fig.3, it shows that the target trajectories obtained by radar A and radar B tend to be consistent after spatio-temporal alignment. Then transformed trajectories are in the same spatio-temporal coordinate system, and can be effectively used for data fusion. For comparison, we also provide the spatial-temporal alignment results of [25], which uses LS method to solve the alignment equation that involves the registration errors. In the LS estimator algorithm, the relative locations and attitudes (with some biases) of radar A and radar B in the same coordinate system are required to get measurements of rotation matrix and translation vector. And, the premise of LS estimator is that pairs of measures coming from the same target are time synchronous. Therefore, the trajectory pairs of the same target have been synchronized according to the known exact time delay before using the LS algorithm. In this paper, space and time registration parameters can be directly estimated according to the trajectory measurements from radar A and radar B in the respective coordinate system. The information of the locations and attitudes of radars and the delay of the system are not required. Fig.4 - Fig.9 show the alignment error and CRLB for estimated $\alpha,\beta,\gamma,c_1,c_2,c_3$. The alignment error is calculated using 200 independent Monte Carlo simulations. Fig.4 and Fig.5 show that the estimation errors of α and β are less than LS estimator. From Fig.6 - Fig.9, the estimation errors of γ,c_1,c_2 and c_3 are less than LS estimator when the number of samples is large. And when the number of samples is small, the LS estimator is more accurate in calculating γ,c_1,c_2 and c_3. Because the proposed algorithm does not require prior spatial information (i.e.,locations and attitudes of radars) and the time delay, it is more difficult to estimate parameters with very few samples. Figure 10 shows the tracking mean error of the LS estimator and the proposed algorithm at each sampling time (CPI) when the total sampling point is 100. The X-axis in Fig.10 represents each CPI. From Fig. 10, it can be seen that the mean of tracking accuracy of the proposed algorithm is 0.5521m and that of the LS estimator is 0.6151m.

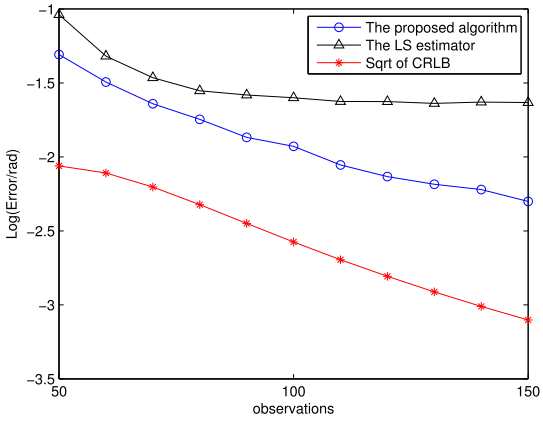

FIGURE 4. Alignment error and CRLB for α.

In the real battlefield environment, the observations of the target movement trajectory from a certain radar may be incomplete due to interference or occlusion. Considering a relatively bad condition, both radar A and radar B are

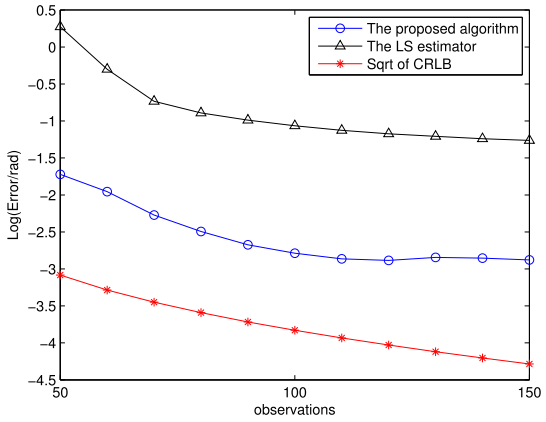

FIGURE 5. Alignment error and CRLB for β.

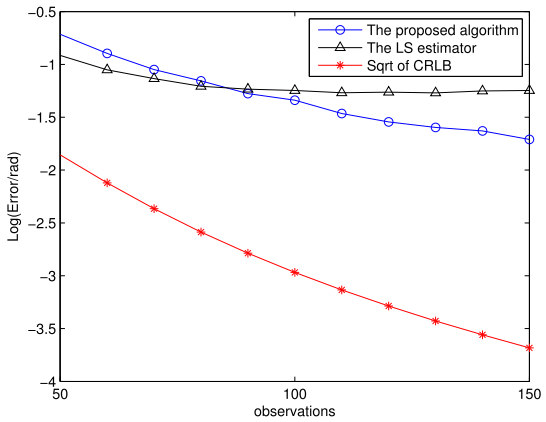

FIGURE 6. Alignment error and CRLB for γ.

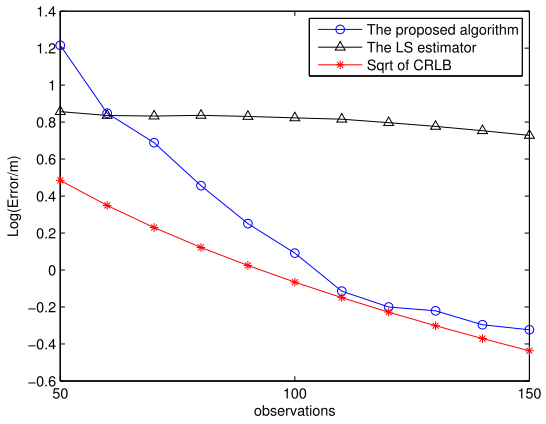

FIGURE 7. Alignment error and CRLB for c_1.

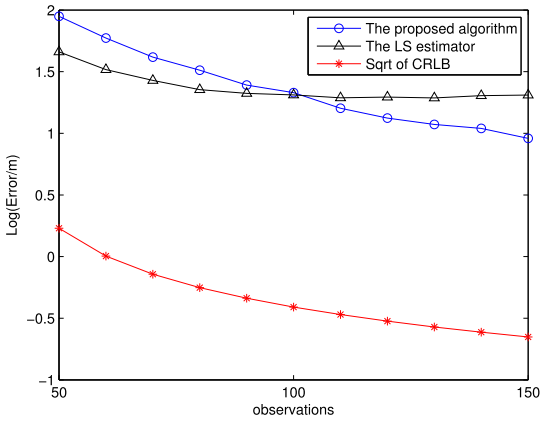

FIGURE 8. Alignment error and CRLB for c_2.

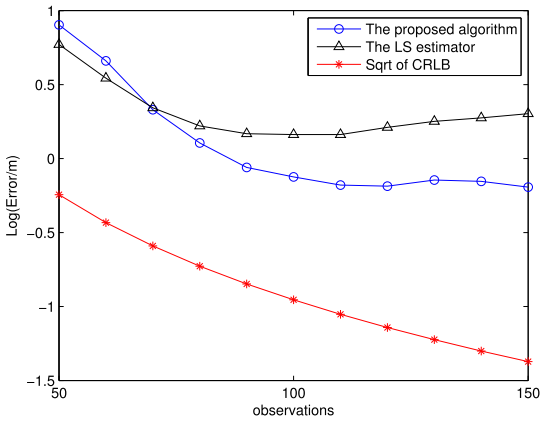

FIGURE 9. Alignment error and CRLB for c_3.

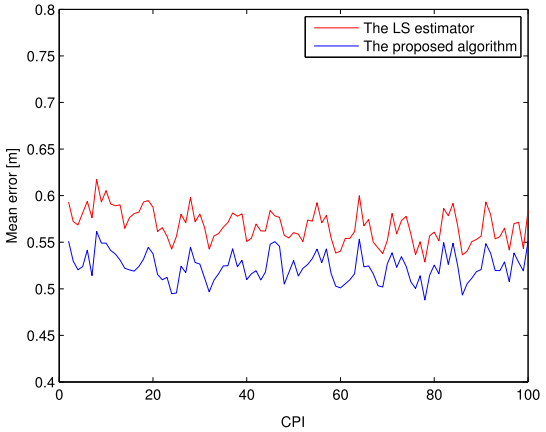

FIGURE 10. Target tracking error of the LS estimator and the proposed algorithm.

occluded, and only part of the target trajectory is observed at some time. The radar A in the geodetic coordinates is [200; 300; 500]. The radar B in the geodetic coordinates is [300; 450; 780]. The detection time of radar A is from $t = 0s$ to $t = 1.8688s$. From $t = 1.8688s$, the radar A starts missing measurements due to interference or occlusion. From $t = 0s$ to $t = 0.4s$, the radar B does not detect the target trajectory due to interference or occlusion. The detection time of radar B is from $t = 0.4s$ to $t = 2.5229s$. In other words, the measurements from radar B has a delay of $\Delta t = 0.4s$ compared with radar A. From $t = 0.4s$ to $t = 1.8688s$, both radar A and radar B detect the target. And part of the trajectories from radar A and radar B overlap during this time, as shown in Fig.11. The green points are the target trajectories that overlap in time from radar A and radar B.

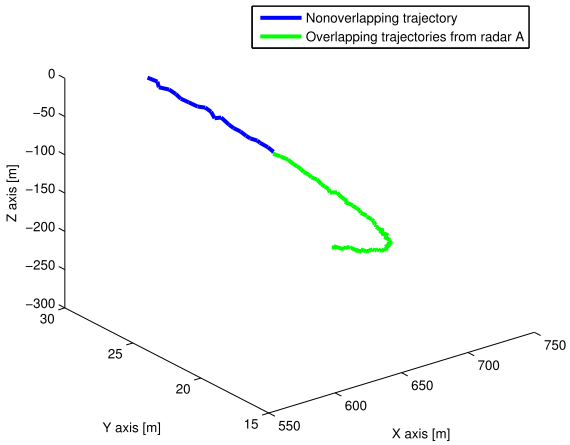

(a)

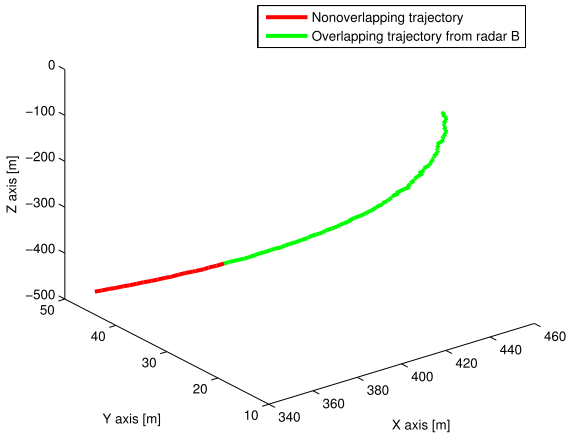

(b)

FIGURE 11. Target trajectory before spatio-temporal alignment. (a) From radar A (b) From radar B.

In practice, when radar A and radar B failed to detect the target and how long the interference affected them are unknown. Because of the interference, the measurements from radar B have an unknown delay Δt compared to radar A. The information when the interference starts and ends is not required. Therefore the starting time of missing measurements is unknown in this algorithm. In this case, the proposed algorithm can be used to align the target trajectory without prior spatial information and time delay, and obtain the complete motion trajectory. The prior information that does not required includes the start time and length of interference, the locations and attitudes of radars. Fig.12 shows the reconstructed target trajectory after alignment. In Fig.12, the blue and red parts represent the track points from radar A and B after alignment. The overlapped part of the red and the blue points is the track part where radar A and radar B are not affected by interference. After spatio-temporal alignment and data fusion, a complete trajectory can be obtained to avoid interference.

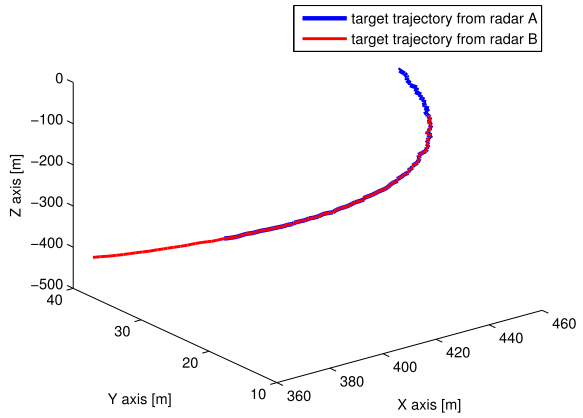

FIGURE 12. Reconstructed target trajectory after fusion.

IV. MATCHING AND ALIGNMENT FOR MULTIPLE TARGETS

A. MATCHING OF MULTIPLE TARGET TRAJECTORIES BASED ON RANSAC

The corresponding relation between trajectories can be established through minimizing sum of paired trajectory error in this paper. It is assumed that data association problem has been solved by classical methods for multi-target case, and we focus on trajectories matching and alignment. In this section, matching and alignment is performed in the multi-target scenario. The spatio-temporal registration for multiple target trajectories can be described in

$$(\mathbf{H}, \mathbf{c}, \Delta t) = \arg\min_{\mathbf{H},\mathbf{c},\Delta t} \sum_{Trajectories} \left(\sum_{i=1}^{N} \left\| \mathbf{q}\left(s \cdot t_i + \Delta t\right) - \left(\mathbf{H} \cdot \mathbf{p}\left(t_i\right) + \mathbf{c}\right) \right\|^2 \right) \tag{49}$$

The algorithm is based on RANSAC and the steps are as follows.

1) M target trajectories are detected and recorded in the spatio-temporal coordinate systems of radar A and B. Measurements of radar A and B are $\mathbf{p}_1(t), \mathbf{p}_2(t), \ldots, \mathbf{p}_M(t)$ and $\mathbf{q}_1(t'), \mathbf{q}_2(t'), \ldots, \mathbf{q}_M(t')$, respectively.

2) A pair of trajectories from radar A and B is randomly chosen to be matched according to the spatio-temporal alignment algorithm for single target in section II. At each trial, the spatio-temporal parameters $(\mathbf{H}, \mathbf{c}, \Delta t)$ which best align the two trajectories are calculated.

3) The estimated parameters are used to transform other trajectories of radar A and radar B. The number of corresponding pairs of trajectories whose distance after alignment is less than a certain threshold is recorded as the matching score for the parameters $(\mathbf{H}, \mathbf{c}, \Delta t)$.

4) Repeat step 2 and step 3 K times.

5) Select the parameters $(\mathbf{H}, \mathbf{c}, \Delta t)$ with the highest score.

6)The alignment parameters are refined using all matched trajectory pairs.

It's worth mentioning that there are two levels of the consistency of spatio-temporal registration: (i) Each radar sensor itself ensures the consistency of the measurements of multiple

target trajectories, which depends on the algorithm of target tracking and trajectories matching used by each radar [28]. (ii) The second level is the consistency of target trajectories between multiple radars. When there are multiple trajectories, the RANSAC (Random Sample Consensus) method adopted in this paper is itself a robust space-time parameter estimation method to maintain consistency. The RANSAC paradigm which is capable of fitting data containing a significant percentage of gross errors is advanced in its effectiveness and efficiency [29]. It has the inherent characteristics of maintaining data consistency and eliminating outliers(unreliable or inconsistent data) effectively.

The first type of consistency is outside the scope of this paper. In order to ensure the the second kind of consistency (the consistency of trajectories between the radars), the threshold in step 3 of RANSAC algorithm should be carefully selected. If the threshold is too large, error sample points may be contained. The threshold cannot be too small either, or there would be too few effective sample points.

B. SIMULATION AND ANALYSIS

LFM waveform of X band is used for simulations and analysis. The time-bandwidth product of the LFM waveform is 24. The radar A in the geodetic coordinates is [200;300;500]. Each measurement cycle contains 4 kinds of LFM waveform with different pulse length, and each CPI contains 256 PRIs. The period of a measurement point is 18.7ms. The radar B in the geodetic coordinates is [300; 450; 780]. Each measurement cycle contains 4 kinds of LFM waveform with different pulse length, and each CPI contains 288 PRIs, The period of a measurement point is 21.0ms. Thus, the ratio between measurement cycle of the radar A and B is $s = 8/9$. The detection time of radar A is from $t = 0s$ to $t = 1.8688s$. From $t = 1.8688s$, the radar A starts missing measurements due to interference or occlusion. From $t = 0s$ to $t = 0.4s$, the radar B does not detect the target trajectory due to interference or occlusion. The detection time of radar B is from $t = 0.4s$ to $t = 2.5229s$. In other words, the measurements from radar B has a delay of $\Delta t = 0.4s$ compared with radar A. From $t = 0.4s$ to $t = 1.8688s$, both radar A and Radar B detect the targets. And part of the trajectories from radar A and radar B overlap during this time, as shown in Fig.13. The green points are the target trajectories that overlap in time from radar A and radar B. Radar A and radar B are characterized by the following measured parameters: i) range accuracy: $\sigma_{\rho,A} = \sigma_{\rho,B} = 1\,m$; ii) azimuth accuracy: $\sigma_{\theta,A} = \sigma_{\theta,B} = 0.01°$; and iii) elevation accuracy: $\sigma_{\varepsilon,A} = \sigma_{\varepsilon,B} = 0.01°$.

M maneuverable targets ($M = 3$ in the example) fly along their respective non-linear trajectories. The first target has an acceleration of 40 m/s^2 in the positive direction of the Y-axis and 60 m/s^2 in the positive direction of the Z-axis. The second target has an acceleration of -10 m/s^2 in the positive direction of the Y-axis and 100 m/s^2 in the positive direction of the Z-axis. The third target has an acceleration of -20 m/s^2 in the positive direction of the Y-axis and -40 m/s^2 in the positive direction of the Z-axis. Radar A and radar B get the targets

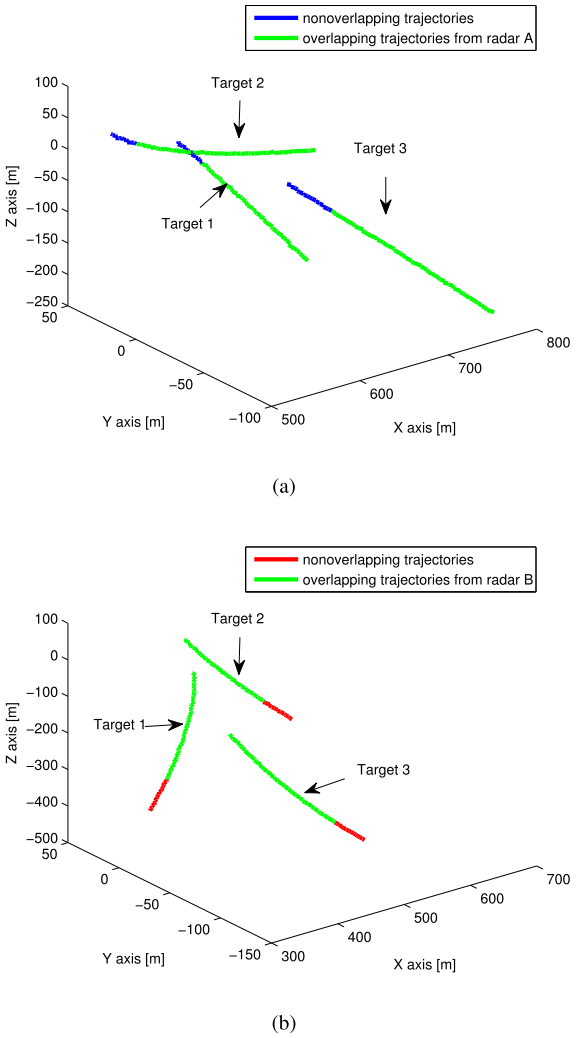

FIGURE 13. Multiple target trajectories before spatio-temporal alignment. (a) From radar A (b) From radar B.

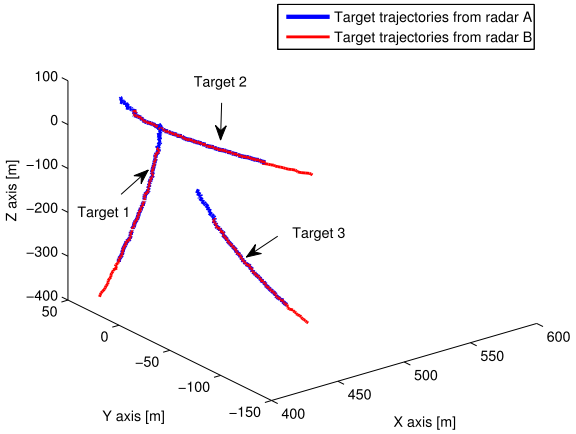

FIGURE 14. Multiple target trajectories after spatio-temporal alignment.

trajectories $\mathbf{p}_1(t)$, $\mathbf{p}_2(t)$, $\mathbf{p}_3(t)$ and $\mathbf{q}_1(t')$, $\mathbf{q}_2(t')$, $\mathbf{q}_3(t')$ in their respective spatio-temporal coordinates, as shown in Fig.13. $\mathbf{p}_1(t)$, $\mathbf{p}_2(t)$, $\mathbf{p}_3(t)$ and $\mathbf{q}_1(t')$, $\mathbf{q}_2(t')$, $\mathbf{q}_3(t')$ all have N observations, and in our simulations $N = 100$.

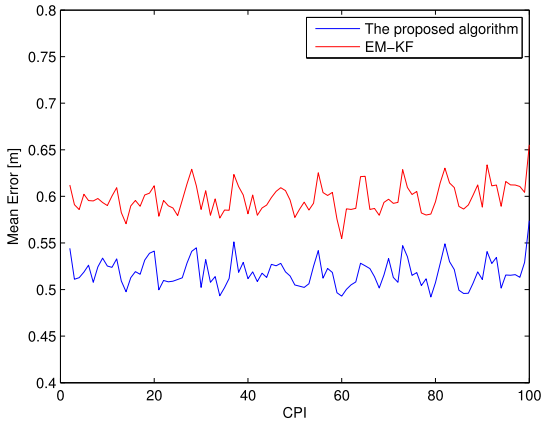

(a)

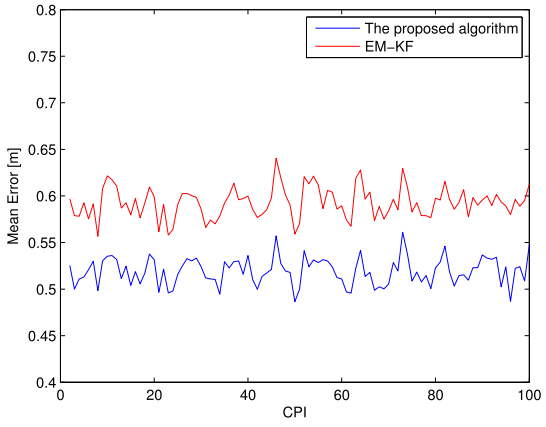

(b)

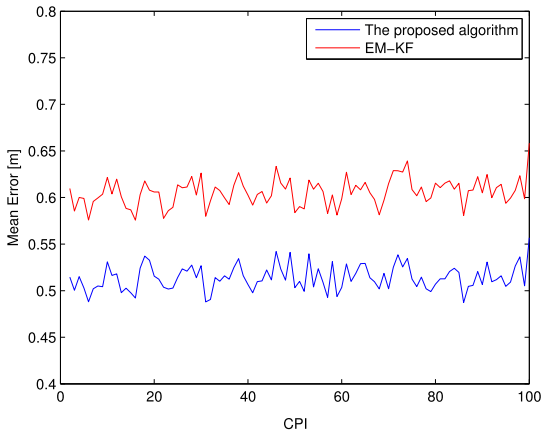

(c)

FIGURE 15. Target trajectory pairs error. (a) Target 1. (b) Target 2. (c) Target 3.

Fig.13 shows that the trajectories of the three targets from radar A and radar B are obtained in the respective spatio-temporal coordinates and multiple targets cannot be matched. Using the method for multiple targets matching proposed in this paper, $(\mathbf{H}, \mathbf{c}, \Delta t)$ with the highest score are obtained as the estimated parameters for spatio-temporal alignment. Then the trajectory pairs supporting the estimated parameters transformation are recorded. As shown in Fig.14, the matching relation of 3 targets is obtained. From Fig.14, we can see that radar A and radar B are in the same spatio-temporal coordinate system after alignment, and the three targets are matched correctly after the multiple targets matching method. With the resulting multiple targets matching relationship, the parameters $(\mathbf{H}, \mathbf{c}, \Delta t)$ are refined by using all matched trajectory pairs.

Fig.15 compares the tracking mean error of the proposed multi-target algorithm with that of the EM-KF algorithm [20] at each sampling time (CPI) when the total sampling point is 100. The X-axis in Fig.15 represents each CPI. The mean error is calculated using 200 independent Monte Carlo simulations. The EM-KF combines expectation-maximization algorithm and the Kalman filter to estimated parameters. The matching and registration parameters are estimated in the M-step of the EM algorithm, and the target states are updated in the condition expectation evaluation in the E-step by KF. The mean errors of the proposed algorithm for target 1, 2, and 3 are 0.5181m, 0.5192m and 0.5140m, respectively. The mean errors of the EM-KF algorithm for target 1, 2, and 3 are 0.5981m, 0.5928m and 0.60590m, respectively. The tracking error of the algorithm proposed in this paper is further reduced than EM-KF algorithm.

V. CONCLUSION

For the spatio-temporal alignment of netted radar, an alternating algorithm is proposed to estimate the spatio-temporal alignment parameters without prior spatial information (including locations and attitudes of radars) and the time delay between radar stations. Multiple targets are matched and aligned by using the RANSAC-based algorithm. With the target information provided by different radar stations, the simulation results show that the algorithm estimates the spatio-temporal alignment parameters effectively. In addition, the correct trajectory matching can be completed for the multiple targets, and the spatio-temporal alignment parameters can be refined with the matched trajectory pairs. And the error of spatio-temporal alignment is further reduced.

REFERENCES

[1] N. Bogdanovic, H. Driessen, and A. G. Yarovoy, "Target selection for tracking in multifunction radar networks: Nash and correlated equilibria," *IEEE Trans. Aerosp. Electron. Syst.*, vol. 54, no. 5, pp. 2448–2462, Oct. 2018.

[2] L. Zafeiriou, E. Antonakos, S. Zafeiriou, and M. Pantic, "Joint unsupervised deformable spatio-temporal alignment of sequences," in *Proc. IEEE Conf. Comput. Vis. Pattern Recognit. (CVPR)*, Jun. 2016, pp. 3382–3390.

[3] W. D. Blair, T. R. Rice, A. T. Alouani, and P. Xia, "Asynchronous data fusion for target tracking with a multitasking radar and optical sensor," *Proc. SPIE*, vol. 1482, pp. 234–246, Aug. 1991.

[4] Y. L. Zhao, X. Z. Ma, X. D. Gao, L. Yun, and S. Q. Fu, "Data fusion algorithm for asynchronous radar networks under blanket jamming," in *Applied Mechanics and Materials*, vol. 157. Stäfa, Switzerland: Trans Tech Publ, 2012, pp. 1446–1452.

[5] G. Tanzmeister and S. Steyer, "Spatiotemporal alignment for low-level asynchronous data fusion with radar sensors in grid-based tracking and mapping," in *Proc. IEEE Int. Conf. Multisensor Fusion Integr. Intell. Syst. (MFI)*, Sep. 2016, pp. 231–237.

[6] X. Rong Li and V. P. Jilkov, "Survey of maneuvering target tracking—Part I. Dynamic models," *IEEE Trans. Aerosp. Electron. Syst.*, vol. 39, no. 4, pp. 1333–1364, Oct. 2003.
[7] B. Ristic, D. E. Clark, and N. Gordon, "Calibration of multi-target tracking algorithms using non-cooperative targets," *IEEE J. Sel. Topics Signal Process.*, vol. 7, no. 3, pp. 390–398, Jun. 2013.
[8] X. Lin, Y. Bar-Shalom, and T. Kirubarajan, "Multisensor-multitarget bias estimation for general asynchronous sensors," *IEEE Trans. Aerosp. Electron. Syst.*, vol. 41, no. 3, pp. 899–921, Jul. 2005.
[9] R. P. S. Mahler, "Multitarget bayes filtering via first-order multitarget moments," *IEEE Trans. Aerosp. Electron. Syst.*, vol. 39, no. 4, pp. 1152–1178, Oct. 2003.
[10] Y. Vershinin and M. West, "A new data fusion algorithm based on the continuous-time decentralized Kalman filter," in *Proc. IEE Target Tracking, Algorithms Appl.*, Oct. 2002, pp. 1–16.
[11] A. Burguera, F. Bonin-Font, and G. Oliver, "Towards robust image registration for underwater visual SLAM," in *Proc. Int. Conf. Comput. Vis. Theory Appl. (VISAPP)*, Oct. 2015, pp. 539–544.
[12] C. Guo, X. Tong, S. Liu, S. Liu, X. Lu, P. Chen, Y. Jin, and H. Xie, "High-precision attitude estimation method of star sensors and gyro based on complementary filter and unscented Kalman filter," *ISPRS Int. Arch. Photogramm., Remote Sens. Spatial Inf. Sci.*, vols. XLII–3/W1, pp. 49–53, Jul. 2017.
[13] H. Chen, X. Cheng, C. Dai, and F. Liu, "Robust stability analysis of H_∞-SGQKF and its application to transfer alignment," *Signal Process.*, vol. 117, pp. 310–321, Dec. 2015.
[14] Y. Zhou, H. Leung, and P. C. Yip, "An exact maximum likelihood registration algorithm for data fusion," *IEEE Trans. Signal Process.*, vol. 45, no. 6, pp. 1560–1573, Jun. 1997.
[15] H. Y. D. Yunlong, H. You, and W. Guohong, "A modified exact maximum likelihood registration algorithm," in *Proc. 3rd Int. Conf. Comput. Electromagn. Appl. (ICCEA)*, Nov. 2004, pp. 85–88.
[16] H. Karniely and H. T. Siegelmann, "Sensor registration using neural networks," *IEEE Trans. Aerosp. Electron. Syst.*, vol. 36, no. 1, pp. 85–101, Jan. 2000.
[17] K. A. Kramer, S. C. Stubberud, and J. A. Geremia, "Target registration correction using the neural extended Kalman filter," *IEEE Trans. Instrum. Meas.*, vol. 59, no. 7, pp. 1964–1971, Jul. 2010.
[18] J. H. Pan and J. Z. He, "On-line absolute sensor registration in 3-D radars networking," in *Proc. Cross Strait Quad-Regional Radio Sci. Wireless Technol. Conf.*, Jul. 2011, pp. 1085–1089.
[19] Z. Li and H. Leung, "An expectation maximization based simultaneous registration and fusion algorithm for radar networks," in *Proc. Can. Conf. Electr. Comput. Eng.*, May 2006, pp. 31–35.
[20] Z. Li, S. Chen, H. Leung, and E. Bosse, "Joint data association, registration, and fusion using EM-KF," *IEEE Trans. Aerosp. Electron. Syst.*, vol. 46, no. 2, pp. 496–507, Apr. 2010.
[21] W. Li, Y. Jia, J. Du, and F. Yu, "Gaussian mixture PHD filter for multisensor multi-target tracking with registration errors," *Signal Process.*, vol. 93, no. 1, p. 86—99, 2013.
[22] W. Wu, J. Jiang, W. Liu, X. Feng, L. Gao, and X. Qin, "Augmented state GM-PHD filter with registration errors for multi-target tracking by Doppler radars," *Signal Process.*, vol. 120, pp. 117–128, Mar. 2016.
[23] T. Zhang, H. Li, L. Yang, W. Liu, and R. Wu, "Multi-radar bias estimation without a priori association," *IEEE Access*, vol. 6, pp. 44616–44625, 2018.
[24] R. E. Helmick and T. R. Rice, "Removal of alignment errors in an integrated system of two 3-D sensors," *IEEE Trans. Aerosp. Electron. Syst.*, vol. 29, no. 4, pp. 1333–1343, 1993.
[25] S. Fortunati, A. Farina, F. Gini, A. Graziano, M. S. Greco, and S. Giompapa, "Least squares estimation and Cramér–Rao type lower bounds for relative sensor registration process," *IEEE Trans. Signal Process.*, vol. 59, no. 3, pp. 1075–1087, Mar. 2011.
[26] S. Umeyama, "Least-squares estimation of transformation parameters between two point patterns," *IEEE Trans. Pattern Anal. Mach. Intell.*, vol. 13, no. 4, pp. 376–380, Apr. 1991.
[27] A. Hjorungnes and D. Gesbert, "Complex-valued matrix differentiation: Techniques and key results," *IEEE Trans. Signal Process.*, vol. 55, no. 6, pp. 2740–2746, Jun. 2007.
[28] A. T. Kamal, J. A. Farrell, and A. K. Roy-Chowdhury, "Information consensus for distributed multi-target tracking," in *Proc. IEEE Conf. Comput. Vis. Pattern Recognit.*, Jun. 2013, pp. 2403–2410.
[29] S.-W. Yang, C.-C. Wang, and C.-H. Chang, "RANSAC matching: Simultaneous registration and segmentation," in *Proc. IEEE Int. Conf. Robot. Autom.*, May 2010, pp. 1905–1912.

XIAOYU CONG was born in 1991. She received the M.S. degree from the School of Information and Control Engineering, China University of Mining and Technology. She is currently pursuing the Ph.D. degree with the Department of Communication and Information System, Nanjing University of Science and Technology. Her current research interests include radar signal processing, information registration, and fusion.

YUBING HAN (Member, IEEE) was born in 1971. He received the Ph.D. degree in signal and information processing from Southeast University, China, in 2006. From 2007 to 2009, he was a Postdoctoral Researcher with the Department of Electronic Engineering, Nanjing University of Science and Technology (NJUST), Nanjing, China. Since 2006, he has been a Faculty Member with the School of Electronic and Optical Engineering, NJUST, where he is currently a Professor. From 2009 to 2010, he was a Visiting Scholar with the Department of Electrical and Computer Engineering, Brigham Young University, Provo, UT, USA. His current research interests include array signal processing, radar signal processing, wireless communications, and digital image processing.

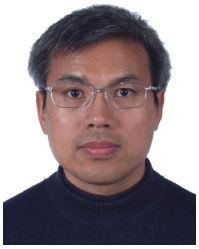

WEIXING SHENG was born in 1966. He received the B.S. degree from the Department of Electronic Engineering, Shanghai Jiaotong University, China, in 1988, the M.S. degree from the Department of Communication and Information System, in 1991, and the Ph.D. degree from the Department of Electromagnetic Field and Electromagnetic Waves, Nanjing University of Science and Technology, China, in 2002. He is current a Professor with the School of Electronic and Optical Engineering, Nanjing University of Science and Technology. So far, he has published more than 40 articles on the IEEE TRANSACTION ON AEROSPACE AND ELECTRONIC SYSTEMS (AES), the IEEE TRANSACTION ON ADVANCED TELECOM COMPUTING ARCHITECTURE (ATCA), and other conferences held in domestic or abroad. He has led various academic and industrial research projects on new radar architectures, radar anti-jamming, and target modeling. His current research interests include radar signal processing, sensor array signal processing, modeling and application of electromagnetic scattering, and image processing.

SHANHONG GUO was born in 1969. She received the Ph.D. degree from the Department of Communication and Information System, Nanjing University of Science and Technology. Her current research interests include radar signal processing and communication and information systems.

RENLI ZHANG (Member, IEEE) was born in 1986. He received the B.S. degree in electronic information engineering and the Ph.D. degree in communication and information system from the Nanjing University of Science and Technology, China, in 2008 and 2013, respectively. He is currently an Associate Professor with the School of Electronic and Optical Engineering, Nanjing University of Science and Technology. His research interests include radar signal processing, netted radar, and digital beamforming.